

Article

# Effect of Expanded Perlite in the Brick Mixture on the Physicochemical and Thermal Properties of the Final Products

Ioannis Makrygiannis \*  and Athena Tsetsekou

School of Mining Engineering and Metallurgy, National Technical University of Athens, Zografou Campus, 15780 Athens, Greece; athtse@metal.ntua.gr

\* Correspondence: ymakrygiannis@sabo.gr

**Abstract:** Thermal insulation is an efficient solution to reduce energy consumption. A great way to reduce the energy consumption of a building is the use of thermal insulation bricks which provide fire resistance and a remarkable thermal capacity, which make them a unique building material for energy efficient buildings. In this study, a fine grain size of expanded perlite was used as additive in a ceramic mass. Brick solid samples were produced from three different mixtures with different ratios of expanded perlite in the mass. From every mixture, three different vacuum values were used. The constructed brick samples were dried and fired in the same conditions and their properties such as bending strength, density and thermal insulation were gathered for six different peak temperatures. The thermal insulation coefficient of every constructed mixture was calculated according to EN1745. It was found that the addition of perlite when keeping the other parameters constant led to decreases in products' density by 2.9% up to 7.1% and in the thermal conductivity coefficient by 5.4% up to 9.5%, confirming that expanded perlite is a very good porogen material. The bending strength also decreased by 18% up to 28%, but in all cases, it remained well above the minimum accepted value of 100 kp/cm<sup>2</sup>. The vacuum employed during extrusion proved an important parameter affecting the results; however, its effect proved less significant as the perlite percentage in the mixture increased.

**Keywords:** expanded perlite; thermal insulation; additives in ceramic mass



**Citation:** Makrygiannis, I.; Tsetsekou, A. Effect of Expanded Perlite in the Brick Mixture on the Physicochemical and Thermal Properties of the Final Products. *J. Compos. Sci.* **2022**, *6*, 211. <https://doi.org/10.3390/jcs6070211>

Academic Editor: Francesco Tornabene

Received: 13 June 2022

Accepted: 15 July 2022

Published: 17 July 2022

**Publisher's Note:** MDPI stays neutral with regard to jurisdictional claims in published maps and institutional affiliations.



**Copyright:** © 2022 by the authors. Licensee MDPI, Basel, Switzerland. This article is an open access article distributed under the terms and conditions of the Creative Commons Attribution (CC BY) license (<https://creativecommons.org/licenses/by/4.0/>).

## 1. Introduction

Fired clay bricks are one of the oldest known building materials and are resistant to harsher weather conditions, which makes them a more reliable brick for use in permanent buildings. The properties of the final product such as mechanical, physical and thermal properties depend on the mineral composition of the raw materials and on the peak firing temperature used [1]. For the improvement of traditional clay bricks, an important parameter is the thermal properties of the final product. The diverse climatic conditions from country to country create a variety of needs regarding the thermal properties of clay building materials. In this respect, P. Foraboschi and A. Vanin [2,3] analyzed how moisture and salts affect the mechanical characteristics of bricks, such as compression strength, that are used in masonry buildings. Furthermore, it is well known that the process environment in a brick factory has the potential to change the physical properties of the manufactured brick products of the same raw material, product size and the technological parameters [4].

Many additives are used in ceramic products. Some are used to create porosity and reduce the drying sensitivity [5] and others to lower the melting point [6] and create an increase in density to achieve acoustic insulation and vitrification of the surface resulting in a reduction in the water absorption of the constructed product.

One of the main targets of the brick and tile industry is to introduce products with appropriate thermal properties. Pore-forming additives in the ceramic mass of a clay brick are expected to provide higher porosity, indicating better thermal behavior. Various studies were carried out to identify additives which burn out during the firing procedure; it was

found that the addition of additives may not exceed 10 *v/v*% due to the reduction in the strength of the final products [7–9].

Due to this fact, this study focused on an additive which does not burn out during the firing procedure and is stable in the ceramic mass of the clay brick. Therefore, taking into consideration the local and traditional materials, ease of transportation, environmental issues and diversity, fine expanded perlite was investigated. Expanded perlite is a lightweight solid agent with remarkable thermo-acoustic qualities. Perlite is an inorganic siliceous ore. The distinguishing feature of perlite is its expansibility of approximately ten (10) times when heated over 800 °C. Perlite contains crystallized water that is evaporated when heated creating numerous microscopic air hollows that provide the insulation characteristics. The LBD (Loose Bulk Density) of dry perlite is approximately 1–1.1 tons/m<sup>3</sup>, whereas the LBD of the expanded perlite may be in the range of 60–500 Kg/m<sup>3</sup> according to the end usage [10]. The countless micropores of dry air in the structure makes the material a very good natural insulator itself. The use of expanded perlite as additive in ceramic mass should improve the insulation properties of clay bricks by creating pores on the brick mass, thereby decreasing the final weight.

Different studies have been carried out to mix expanded perlite in the ceramic mass of a clay brick. Hamza and Kocserha (2020) [1] added expanded perlite 30–45 *v/v*% type ANZO P2 and compared the mechanical properties such as drying and firing shrinkage, absorption, and density with the addition of sawdust. Thus, the authors found that the amount of expanded perlite does not increase the water absorption and enhances the frost resistant of the final products. Chaouki Sadik et al. (2013) [11] examined the use of expanded perlite in the ceramic mass combined with recycled factory waste. The additions of perlite were 10%, 20% and 30% *v/v* and it was reported that the strength of the final products becomes extremely low; therefore, the further addition of additives is not recommended.

Expanded perlite, however, is not a material that can be found in abundance in nature; it requires processing to be constructed or can be purchased from a brick factory and requires a line of mixing with the clay material to form a homogeneous mixture to produce new products [12]. This line can consist of a silo, box feeder, stirring line with clay materials, etc. which can be costly. In addition, the extruders in brick and tile industries use high pressures to shape the production clay material into wet bricks. The pressure developed during extrusion may affect the properties of the expanded perlite in the mass of the final product and could lead to undesired results.

For this reason, this study aimed to investigate the following three key-factor characteristics of the final products:

- Density;
- Bending strength;
- Thermal conductivity of the final product.

The testing procedure employed in the study attempted to simulate the extrusion of a real brick factory on a pilot scale in the laboratory, with the main purpose of recording how the extrusion pressure affects the final product in combination with the percentage of perlite added to the mass.

The final aim of the whole study was to evaluate the required economic investment for such a venture. The efflorescence phenomenon of the constructed samples from all mixtures was also determined.

Consequently, expanded perlite with small grain sizes was used as additive in the ceramic mass in different ratios while applying different vacuum values for the extrusion properties. Within this scope, the constructed samples from clay and perlite mixtures were compared with the samples from pure clay material tested in the same preparation, extruding, drying, and firing process environment.

## 2. Materials and Methods

### 2.1. Characteristics of Clay

The typical clay type used in the industrial brick production in the Evia region was used in this study. The properties of the clay coded as TZ can be seen in Table 1. According to ISO 14688-2:2017, TZ is an inorganic clay with medium plasticity since the liquid limit is in the range of 35–50%. The chemical composition of the clay was determined via Atomic Absorption Spectrometry (AAS) according to ISO 26845:2016 and is shown in Table 2. The AVGUSTINIK-diagram may contribute to assessing the suitability of the TZ clay based on the chemical analysis shown in Figure 1. The particle size of the clay was analyzed according to ASTM D422-63 (2007), [13]. The particle size distribution of TZ can be seen in Figure 2 which indicated a particle size range from 2 mm to 2 μm. The average humidity content of the clay brought from the manufacturing site to the laboratory was 8.15 wt%, and the average density of the clay was 1781 Kg/m<sup>3</sup> according to ASTM D698-12 [14]. XRD diffractograms of TZ clay are provided in Figure 3 which define the mineralogical composition. The implementation of XRD was achieved by using Siemens D500 Powder Diffractometer. According to the XRD analysis, the clay consists of quartz, calcite, manganoan calcite, kaolinite, Potassium aluminum silicate, Chlorite, Palygorskite, Anorthite and Moganite.

Table 1. Physical properties of TZ clay.

Physical Properties	Unit	Values
Plastic Limit [15]	% (wt.)	20.76
Liquid limit [15]	%	42.00
Plasticity [15]	%	24.23
Density	Kg/m <sup>3</sup>	1781

Table 2. Oxide composition of TZ clay.

Oxides (%)	SiO <sub>2</sub>	Al <sub>2</sub> O <sub>3</sub>	CaO	Fe <sub>2</sub> O <sub>3</sub>	MgO	K <sub>2</sub> O	Na <sub>2</sub> O	LOI
TZ clay	56.45	16.72	5.65	5.08	2.73	1.64	0.55	9.34

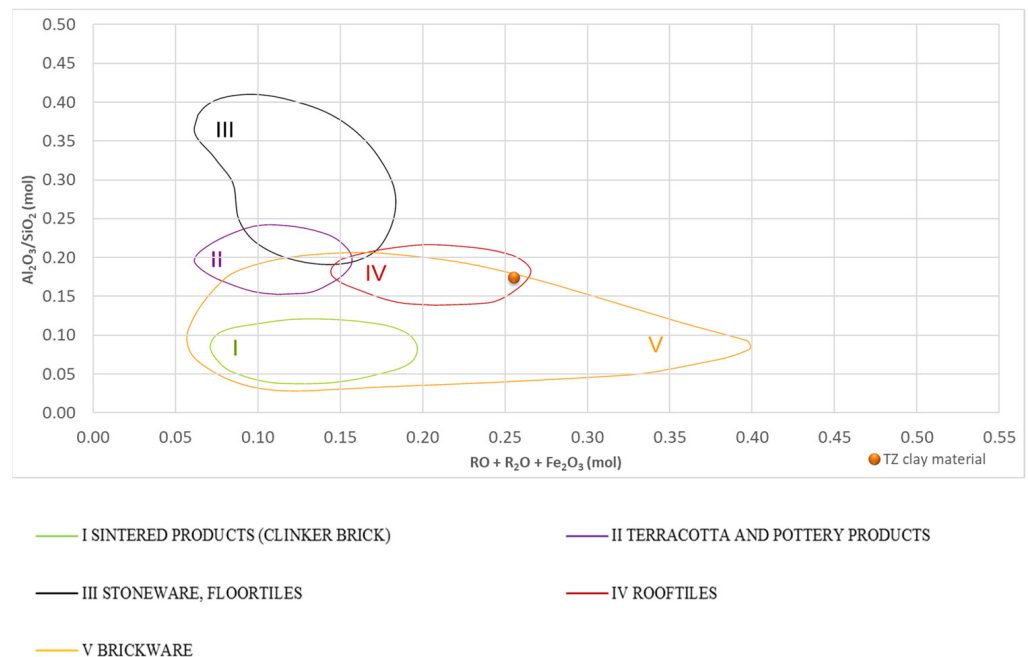


Figure 1. Suitability according to AVGUSTINIK of TZ clay [16].

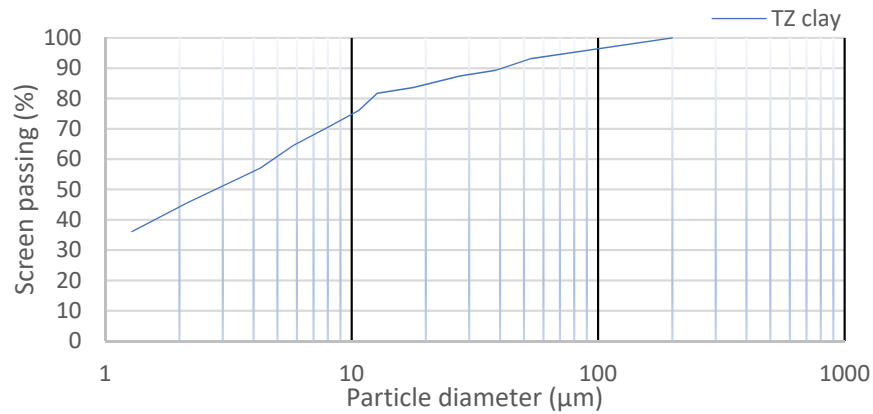


Figure 2. Particle size distribution of TZ clay.

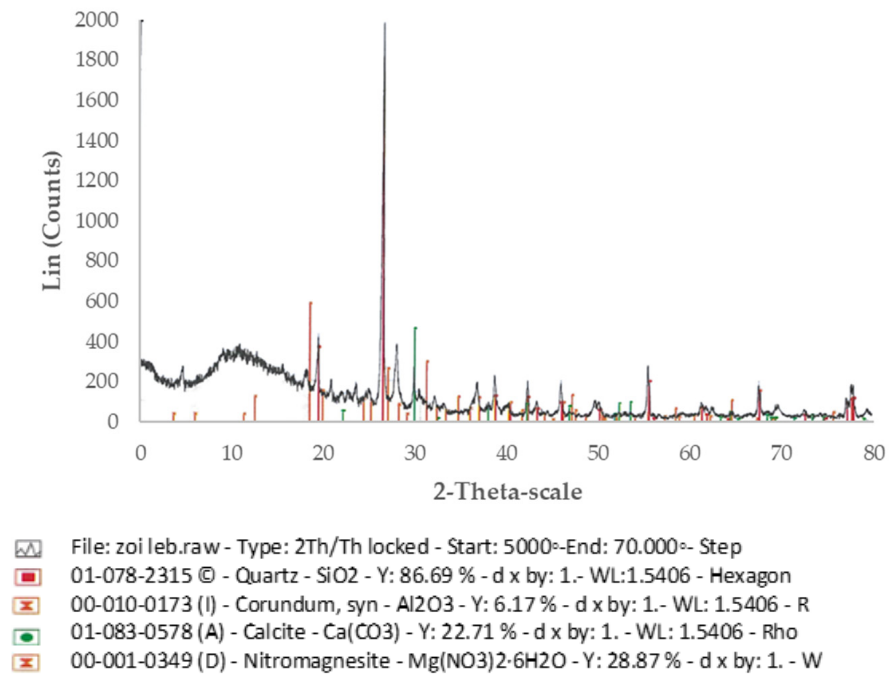


Figure 3. XRD diffractograms of TZ clay.

2.2. Characteristics of Expanded Perlite

The expanded perlite used for the implementation of the testing procedure was fine expanded perlite GEOMIN A2, with grain sizes of 0.25–1 mm and a loose bulk density of 60 Kg/m<sup>3</sup>. The chemical composition and the physical properties of the perlite can be seen in Tables 3 and 4, respectively.

Table 3. Oxide composition of perlite.

Oxides (%)	SiO <sub>2</sub>	Al <sub>2</sub> O <sub>3</sub>	CaO	Fe <sub>2</sub> O <sub>3</sub>	MgO	K <sub>2</sub> O	Na <sub>2</sub> O	LOI
Perlite	76.0	13.2	1.0	1.2	0.5	2.5	0.5	4.0

Table 4. Physical properties of perlite.

Color	Odor	Bulk Density	Specific Gravity	Moisture	PH	Softening Point	Active Silica
		Kg/m <sup>3</sup>		%		°C	%
White/gray	Odorless	575	2.2	Max 1	7.5	870–1000	49.22

### 2.3. Methodology

The methodology followed in the laboratory was a simulation of the process environment for industrial-scale brick production. For the laboratory tests, 75 kg of representative clay samples from a brick and tile factory in the region of Evia was gathered according to DIN 51061 (part 2). The determination of the moisture content was achieved according to DIN 51062 chapter 5.2. The moisture content is the share of water existing in a humid raw material given in percent, whereby the quantity of water refers to the weight of the humid material (wet base). To measure the moisture content, the sample was weighed in a vessel. This sample was dried in the laboratory drying oven at 110 °C until a constant weight was reached, then it was weighed again. The humidity of the obtained sample and the preparation water contents were determined in the same way as the moisture content.

#### 2.3.1. Mixture Preparations

The preparation procedure in the laboratory was similar to the preparation procedure in a brick factory. Before proceeding to the tests, the TZ material was dried in the laboratory electric dryer, SCN/400/DG model, at 110 °C for twenty-four hours. Then, it was ground down using a laboratory jaw crusher model A 92 with the opening of the jaws adjusted at 2 mm. The crushed material was ground further using a laboratory roller mill, type Verdes 080, which features two smooth cylinders that work against each other at different speeds with an adjustable separation of 1 mm.

Three mixtures were constructed with the ground TZ clay with expanded perlite ranging from 0 to 30% *v/v* for three different vacuum indexes. The raw materials were weighted according to their mixing ratio and considering their actual moisture. The mixing of clay and expanded perlite was achieved through a conical rotated mixture model MI/10, for 40 min. Water was added until a satisfactory deformation index (Pfefferkorn's test) was achieved [17].

The water addition is always unique per mixture and depends on the absorptivity of the raw material and the extrusion process that will be followed given the type and quality of the product required. The water addition should always be standard to avoid inhomogeneity problems in mixtures which can lead to differential stresses and subsequent deformations and quality issues during extrusion [18]. The mixture proportions are shown in Table 5.

**Table 5.** Mixture proportions of clay brick samples.

Lab. Code	Exp. Perlite Ratio ( <i>v/v</i> %)	Water Addition on Dry Basis (%)	Plasticity Pfefferkorn
EPTZ020	0	26.65	0.75
EPTZ030	0	26.12	0.75
EPTZ050	0	25.81	0.76
EPTZ2020	20	26.07	0.75
EPTZ2030	20	25.72	0.75
EPTZ2050	20	25.26	0.75
EPTZ3020	30	24.73	0.75
EPTZ3030	30	24.95	0.75
EPTZ3050	30	24.23	0.75

#### 2.3.2. Extruding Procedure

The samples were vacuum-extruded into rectangular specimens of standard dimensions to determine drying and firing properties. The laboratory extruder model used was the HÄNDLE de-airing extrusion unit for laboratory and operation, KHS-Type: PZVM8b and consists of:

A feeding chamber, on top of which there is a porch for material input; and a pre-extruding mixing part which includes a screw mixer that pushes the material through an air-vacuum chamber to the extruding output. There is also a vacuum pressure gauge to monitor

the pressure under which the clay is being extruded. The clay is fed into the machine manually from the top. At the output, the outer extruding part can receive interchangeable molds that are constructed to fit the desired size and shape of the products extruded.

The samples were rectangular solid samples and extruded with a size of  $120 \times 20 \times 20$  mm. In total, 180 samples were constructed, with 20 used per tested procedure (3 mixtures  $\times$  3 vacuum indexes  $\times$  20 samples). The vacuum extruder and the die are shown in Figure 4.



**Figure 4.** The extruder and the sample mouth of the extruder.

The 3 constructed mixtures with expanded perlite and TZ clay were extruded with 3 standard vacuum pressures which on extrusion reached 0.9, 0.8 and 0.7  $\text{kp}/\text{cm}^2$ , as can be seen in Table 6.

**Table 6.** Mixture proportions of clay brick samples.

Lab. Code	Exp. Perlite Ratio	Vacuum Pressure
	(v/v%)	Kp/cm <sup>2</sup>
EPTZ020	0	0.7
EPTZ030	0	0.8
EPTZ050	0	0.9
EPTZ2020	20	0.7
EPTZ2030	20	0.8
EPTZ2050	20	0.9
EPTZ3020	30	0.7
EPTZ3030	30	0.8
EPTZ3050	30	0.9

### 2.3.3. Drying Procedure

After the extrusion, all samples were placed in the laboratory's electric dryer (type SCN/400/DG) for a smooth drying cycle to prevent damage at increased temperatures [19]. The drying process consisted of 3 different phases. The 3 phases were as follows:

- "Humidity" phase: At the beginning of the process, the ambient humidity was kept at high levels.
- Shrinkage critical point phase: The phase after the critical point, where the drying rate dropped dramatically and shrinkage approached the end.
- Final drying phase: At the end of the drying program, ambient humidity was observed in levels low enough to secure safe firing.

Each phase demanded specific attention during the drying procedure because each phase could raise different issues in terms of the brick samples.

During the "humidity" phase, ambient humidity in the dryer was at high levels in order to keep the surface pores of the bricks open. It was the most critical phase during drying, because cracks, deformations, or fragility of the bricks may occur. During the

“shrinkage critical point phase” the drying shrinkage was completed before the temperature rose rapidly to complete drying. In this phase, the temperature increase occurred gradually to avoid cracking issues. In the last phase, the aim was to reduce the remaining body humidity in the brick samples as much as possible (Figure 5).



**Figure 5.** Dried samples before being placed to the electric laboratory kiln.

#### 2.3.4. Firing Procedure

All dried samples from the constructed mixtures were fired in the electric gradient kiln of the Laboratory (Nabertherm model GR1300/13). The computer-controlled kiln was set to test 6 different firing temperatures in 8 time-duration steps to ensure adequate preheating, top firing and smooth cooling. Afterwards, the firing process samples were subjected to smooth cooling to avoid cracking [19]. The firing temperatures that were used for the study were 1000 to 830 °C. The rate of increase in the temperature was between 0.7 and 1.16 °C/min, depending on the firing zone. A soaking time of 3 hours was maintained for the maturing temperature. The cooling process required about 15 hours in accordance with the natural heat loss of the kiln. The firing cycle lasted 24 hours from cold to cold and can be seen in Figure 6.

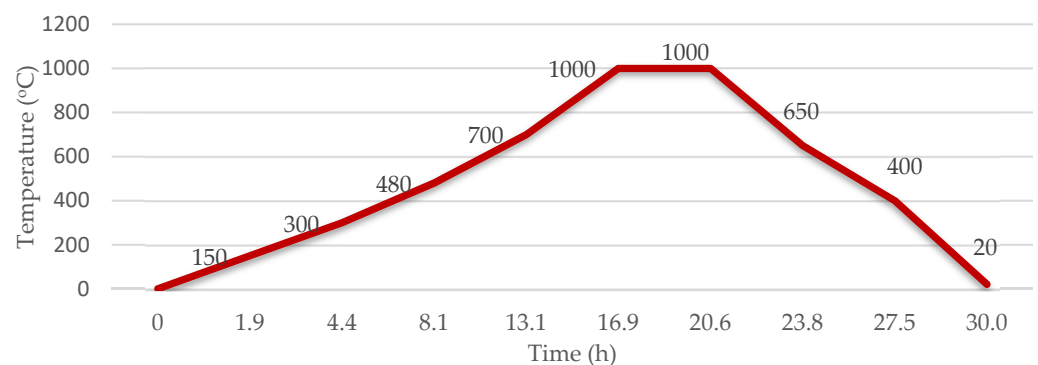


**Figure 6.** The firing cycle of the brick samples.

No problems such as cracks, surface detachments or deformations were faced during the firing cycle, indicating that the process environment that was followed during the tests was successful.

The firing time and the atmosphere of the individual program steps simulated those of the factory’s which provide the TZ clay for testing. This was also the case with the firing tests in the shrinkages and the water absorption of the ore determined after firing, and the firing results were evaluated.

### 2.3.5. Properties Characterization

The linear drying shrinkage and firing linear shrinkage were measured in accordance with the standard ASTM C326-09 [20]. The Archimedes method based on ASTM C373-14a [21] was used to determine the bulk density and water absorption. The bending strength of the fired samples was measured in test specimens with dimensions of  $120 \times 20 \times 20$  mm. A three-point bending test device with a distance of 100 mm between the bearings was used for this purpose and 3 test specimens from each composition/production method were tested (Figure 7). The compressive strength of the fired products was determined according to ASTM C 648-20 [22]. The thermal coefficient ( $\lambda$  10, dry, mat) of the fired clay samples was calculated according to the EN1745:2012 [23].



**Figure 7.** Fired samples for mixture EPTZ3050 before and after the evaluation of the bending strength on fired products.

To calculate the water content after drying, 15 test samples from every preparation procedure, with dimensions of  $120 \times 20 \times 20$  mm, were weighted directly after shaping and dried in the laboratory's oven using a twenty-four (24) hours drying cycle as described above. The preparation water content was calculated from the wet and dry weight according to the following formula:

$$WR = \frac{\text{Weight of wet} - \text{Weight of dry}}{\text{Weight of dry}} * 100 \quad (1)$$

In order to avoid any misunderstandings, the weight of the dry specimens was used as a reference throughout.

To evaluate the shrinkage percentage, shrinkage markings were applied to the test samples in the clay column direction and lateral to the clay column. The markings were evaluated after drying and again after firing to determine the drying shrinkage and total shrinkage (wet to fired).

## 3. Results

### 3.1. Drying Procedure

All the specimens from all the mixtures were dried in the same conditions. For each mixture, the average of 10 samples was taken. Drying shrinkage decreased as the addition of expanded perlite increased and as the vacuum pressure increased too. Based on the results, the lowest drying shrinkage was found in the mixture with 30% *v/v* expanded perlite and a vacuum pressure of 0.9 Kp/cm<sup>2</sup>. The drying shrinkage from all mixtures can be seen in detail in Figure 8.



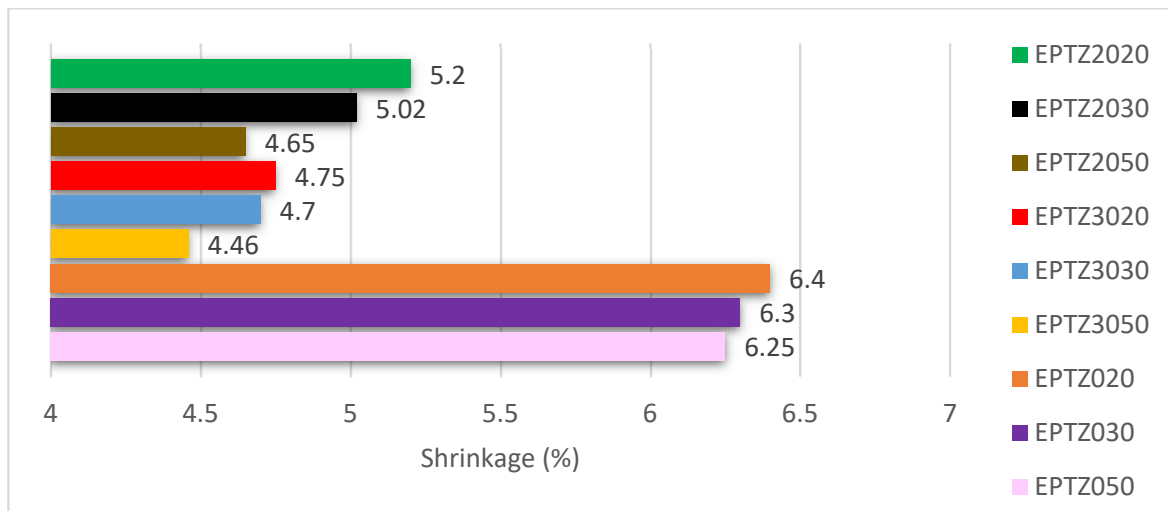


**Figure 8.** Drying shrinkage for all the constructed mixtures.

### 3.2. Bulk Density and Water Absorption

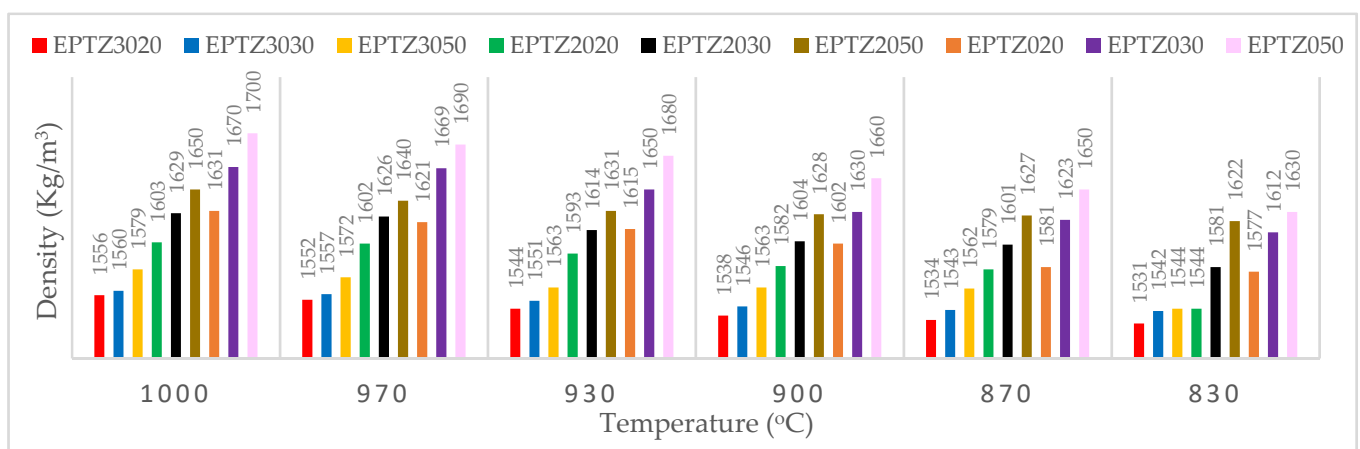
Based on Archimedes' Law, all the constructed samples were tested via bulk density and water absorption. The highest density,  $1700 \text{ Kg/m}^3$ , was found in the additive-free samples with the highest vacuum pressure and at the highest tested peak temperature ( $1000 \text{ }^\circ\text{C}$ ). With the incorporation of additives, the bulk density of the samples showed a decrease in all cases. The lowest bulk density,  $1531 \text{ Kg/m}^3$ , was found in the samples with the highest additive ratio (30%), lowest extruded pressure and the lowest tested peak temperature ( $830 \text{ }^\circ\text{C}$ ). Based on the results obtained, the increasing vacuum index of the extruder significantly affected the mixture with the lower amount of expanded perlite. The increase in the vacuum index increased the density of the samples produced from the mixture without perlite by 4% irrespective of the peak firing temperature. For the mixture with 20% expanded perlite in the mass, the density increased in all sintering temperatures by 2% and for the mixture with 30% expanded perlite in the mass, it increased by 1.4%. Therefore, it can be derived that as the perlite addition in the mass increases, the final sample density is affected less by the vacuum index. The increase in the density with the vacuum index can be attributed to the crushing of expanded perlite which intensifies as the vacuum increases due to the rise of pressure among the mixture particles. When the expanded perlite particles are crushed by soil particles, the air content is lost, and the perlite becomes inert. This fact results in porosity not increasing to the desired level and accordingly the density not decreasing as expected—a phenomenon that is attenuated as the expanded perlite in the mixture increases.

This observation was confirmed by examining the results obtained for the different mixtures after firing at the same peak temperature. The mixture with 30% expanded perlite presented a 1.58% higher density in a  $0.9 \text{ kp/cm}^2$  vacuum index compared to that obtained in  $0.7 \text{ kp/cm}^2$ . For the mixture with 20% expanded perlite in the mass, the density increase in the respective vacuum index values was 2.85% and for 100% clay material this increase was 4.1%.

Another important observation was the tested peak temperature which was found to affect the density independently of the addition of the expanded perlite content. All tested samples presented an increase of 3 to 3.5% in density from peak temperatures of  $830$  to  $1000 \text{ }^\circ\text{C}$ . This result was expected as the increase in firing temperature promotes sintering and densification processes in ceramic masses. All the density results can be seen in Table 7.

**Table 7.** Bulk density of the tested samples.

Mixtures	Kp/cm <sup>2</sup>	Density of Final Products (kg/m <sup>3</sup> ) in Different Firing Peak Temperatures						Laboratory Code for Mixture
		1000 °C	970 °C	930 °C	900 °C	870 °C	830 °C	
70–30%	0.7	1556	1552	1544	1538	1534	1531	ERTZ3020
	0.8	1560	1557	1551	1546	1543	1542	ERTZ3030
	0.9	1579	1572	1563	1563	1562	1544	ERTZ3050
80–20%	0.7	1603	1602	1593	1582	1579	1544	ERTZ2020
	0.8	1629	1626	1614	1604	1601	1581	ERTZ2030
	0.9	1650	1640	1631	1628	1627	1622	ERTZ2050
100% TZ	0.7	1631	1621	1615	1602	1581	1577	ERTZ020
	0.8	1670	1669	1650	1630	1623	1612	ERTZ030
	0.9	1700	1690	1680	1660	1650	1630	ERTZ050



The water absorption capacity results were in accordance with the density results, with the lowest density results presenting higher absorption capacity values. These results can be seen in Table 8. A general conclusion is that the vacuum index affects density and consequently porosity and water absorption.

**Table 8.** Absorption for all constructed mixtures at 6 different temperatures.

Mixtures	Kp/cm <sup>2</sup>	Absorption of Final Constructed Products (%) in Different Peak Temperatures for Every Constructed Mixture.						Laboratory Code for Mixture
		1000 °C	970 °C	930 °C	900 °C	870 °C	830 °C	
70–30%	0.7	12.37	13.37	13.49	13.86	14.17	14.19	ERTZ3020
	0.8	12.30	13.01	13.22	13.58	13.87	14.36	ERTZ3030
	0.9	12.21	12.57	12.66	13.63	13.98	14.28	ERTZ3050
80–20%	0.7	12.18	12.86	13.34	13.52	14.09	15.61	ERTZ2020
	0.8	10.65	11.55	11.95	13.45	14.04	14.86	ERTZ2030
	0.9	9.04	9.67	9.98	10.51	12.81	13.71	ERTZ2050
100% TZ	0.7	10.49	11.34	12.17	13.28	14.46	14.89	ERTZ020
	0.8	9.39	10.64	11.89	12.35	13.25	14.56	ERTZ030
	0.9	9.03	9.87	10.52	11.74	12.57	14.12	ERTZ050

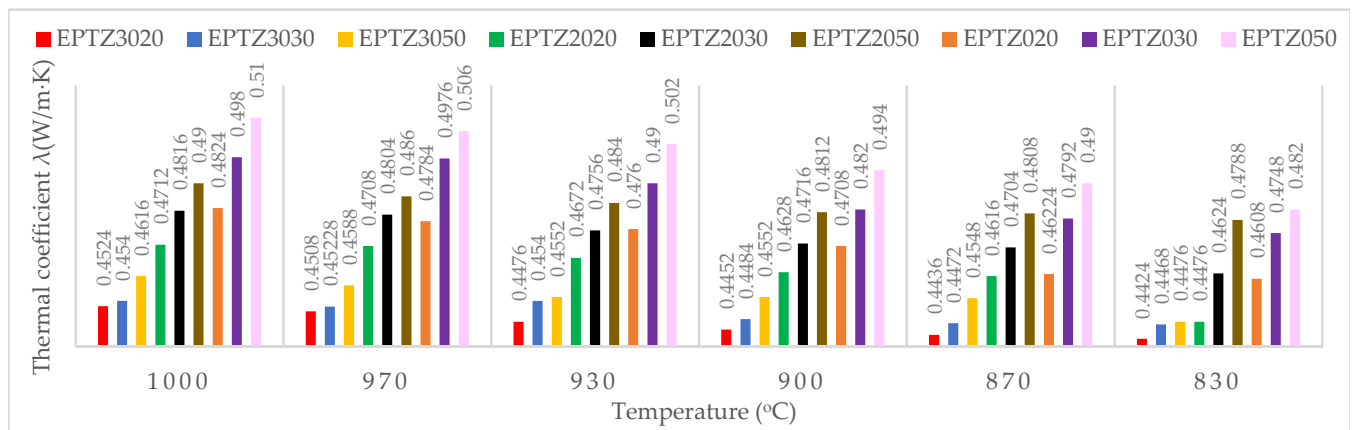
The higher vacuum index employed the lowest absorption obtained after firing at the same temperature. This fact indicates that the vacuum provides strong body cohesion during processing, thereby decreasing the porosity of the final product.

### 3.3. Thermal Conductivity Coefficient

The thermal conductivity coefficient ( $\lambda$ ) tests results obtained from the mixtures are shown in Table 9. The thermal conductivity coefficient decreased significantly with the increase in the expanded perlite. However, the  $\lambda$  value increased as the vacuum pressure increased. Even the brick samples without the addition of expanded perlite in the lowest tested vacuum pressure presented a lower  $\lambda$  value compared with the samples with expanded perlite addition and high vacuum pressure. The thermal conductivity coefficient was affected by the density and the porous structure of the samples. Therefore, both the sintering temperature and the vacuum index affect its value. It is known that the firing temperature significantly affects the physical properties of the clay bricks due to the vitrification of silica at high temperatures [24]. For the minimum tested vacuum pressure and the same temperature of 900 °C, the samples without the addition of expanded perlite presented a lambda ( $\lambda$ ) value of 0.47 W/m·K which decreased to 0.46 W/m·K with the addition of 20% expanded perlite and reached 0.44 W/m·K with the addition of 30% expanded perlite. For the highest tested vacuum pressure samples, the thermal conductivity coefficient values were 0.49 W/m·K for the samples without perlite, 0.48 W/m·K with 20% perlite addition and 0.45 W/m·K with 30% perlite addition. Regarding the above results, and in contrast with the density behavior of the mixtures, the ratio of the expanded perlite added to the ceramic mass was found to significantly affect thermal insulation. The thermal insulation coefficient showed decreased values as the vacuum index decreased, but these values, for 30% addition of expanded perlite, did not differ by more than 1% as the vacuum index decreased from 0.9 kp/cm<sup>2</sup> to 0.7 kp/cm<sup>2</sup>. The difference for the samples with 20% expanded perlite was 1.74% and for the mixtures without perlite addition it was 2.41%. The peak temperature for each sample category led to very small variations in the thermal insulation coefficient with deviations of less than 1%.

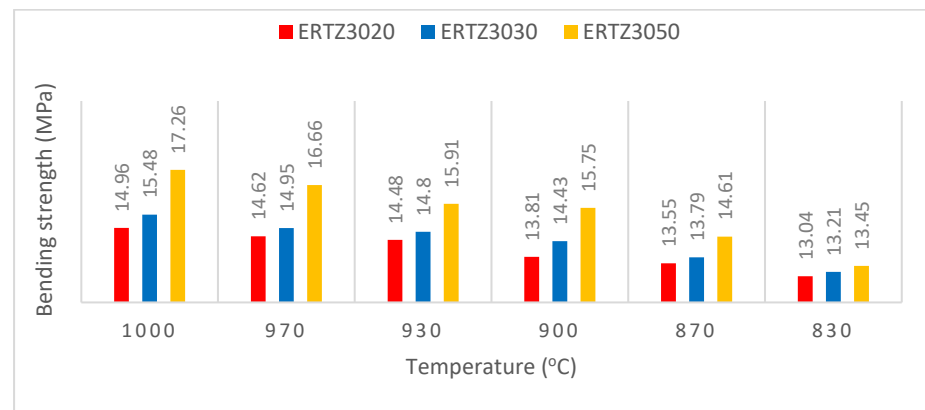
Table 9. Thermal conductivity coefficient of the tested samples.

Mixtures	Kp/cm <sup>2</sup>	Thermal Coefficient of Final Products (W/m·K) in Different Firing Peak Temperatures						Laboratory Code for Mixture
		1000 °C	970 °C	930 °C	900 °C	870 °C	830 °C	
70–30%	0.7	0.452	0.451	0.448	0.445	0.444	0.442	ERTZ3020
	0.8	0.454	0.452	0.454	0.448	0.447	0.447	ERTZ3030
	0.9	0.462	0.459	0.455	0.455	0.455	0.448	ERTZ3050
80–20%	0.7	0.471	0.471	0.467	0.463	0.462	0.448	ERTZ2020
	0.8	0.482	0.480	0.476	0.472	0.470	0.462	ERTZ2030
	0.9	0.490	0.486	0.484	0.481	0.481	0.479	ERTZ2050
100% TZ	0.7	0.482	0.478	0.476	0.471	0.462	0.461	ERTZ020
	0.8	0.498	0.498	0.490	0.482	0.479	0.475	ERTZ030
	0.9	0.510	0.506	0.502	0.494	0.490	0.482	ERTZ050

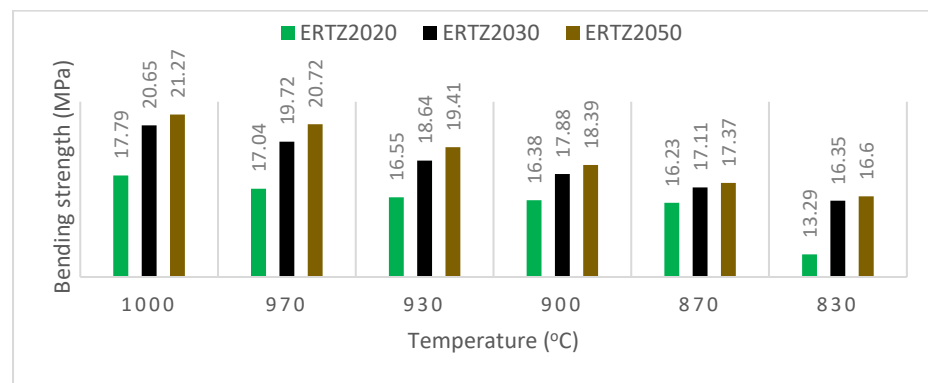


### 3.4. Bending Strength

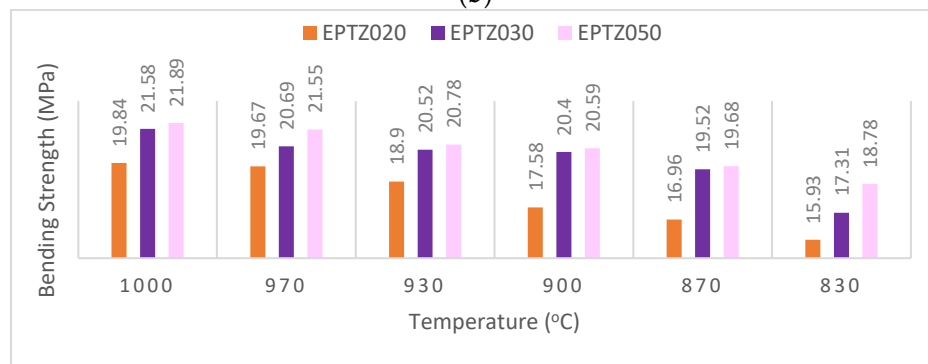
The bending strength values for the as-developed samples are shown in Figure 9a–c. With the increase in the expanded perlite, the strength was shown to decrease. To summarize all the results, the bending strength was shown to depend on the vacuum pressure values (the higher, the better), the peak temperatures (the higher, the better) and the added percentage of the additive (the higher, the lower). It was shown that as the perlite percentage increased, while keeping the other parameters constant, the bending strength decreased from 18% to 28%. The larger deviation was observed when the high vacuum index of 0.9 kp/cm<sup>2</sup> was employed, whereas when the lower vacuum index of 0.9 kp/cm<sup>2</sup> was used this reduction was less pronounced.



(a)



(b)



(c)

**Figure 9.** (a) Bending strength for mixtures with 30% expanded perlite in 6 different peak temperatures, (b) Bending strength for mixtures with 20% expanded perlite in 6 different peak temperatures and (c) Bending strength for mixtures without expanded perlite in 6 different peak temperatures.

#### 4. Discussion

Within the scope of this study, expanded perlite was added to a clay brick production mixture in different amounts and extruded with different vacuum pressure values. The main aim was to create controlled porosity fired bricks and to study the density, the strength and the thermal insulation of the new products. The secondary target was to evaluate how the vacuum pressure affects the final products' properties with and without the addition of expanded perlite. Table 10 summarizes the results described above, allowing for the evaluation of the parameters that mostly affected the properties.

**Table 10.** Summary of results from the constructed mixtures.

Mixture		TC1	TC2	TC3	TC4	TC5	TC6	TC7	TC8	TC9
Laboratory code:		w/v%	w/v%	w/v%	w/v%	w/v%	w/v%	w/v%	w/v%	w/v%
		ERTZ 020	ERTZ 030	ERTZ 050	ERTZ 2020	ERTZ 2030	ERTZ 2050	ERTZ 3020	ERTZ 3030	ERTZ 3050
Material No.1-Clay TZ Exp. perlite (0.25–1 mm)		100	100	100	80	80	80	70	70	70
Vacuum index	Kp/cm <sup>2</sup>	0	0	0	20	20	20	30	30	30
		0.7	0.8	0.9	0.7	0.8	0.9	0.7	0.8	0.9
Firing Temperature	°C	830 *								
Bending strength/fired	Mpa	15.93	17.31	18.78	13.29	16.35	16.6	13.04	13.21	13.45
Body density	Kg/cm <sup>3</sup>	1577	1612	1630	1544	1581	1622	1531	1542	1544
Thermal conductivity ( $\lambda_{eff}$ )	W/m·K	0.461	0.475	0.482	0.448	0.462	0.479	0.442	0.447	0.448
Firing Temperature	°C	870 *								
Bending strength/fired	Mpa	16.96	19.52	19.68	16.23	17.11	17.37	13.55	13.79	14.61
Body density	Kg/cm <sup>3</sup>	1581	1623	1650	1579	1601	1627	1534	1543	1562
Thermal conductivity ( $\lambda_{eff}$ )	W/m·K	0.462	0.479	0.490	0.462	0.470	0.481	0.444	0.447	0.455
Firing Temperature	°C	900 *								
Bending strength/fired	Mpa	17.58	20.40	20.59	16.38	17.88	18.39	13.81	14.43	15.75
Body density	Kg/cm <sup>3</sup>	1602	1630	1660	1582	1604	1628	1538	1546	1563
Thermal conductivity ( $\lambda_{eff}$ )	W/m·K	0.471	0.482	0.494	0.463	0.472	0.481	0.445	0.448	0.455
Firing Temperature	°C	930 *								
Bending strength/fired	Mpa	18.9	20.52	20.78	16.55	18.64	19.41	14.48	14.8	15.91
Body density	Kg/cm <sup>3</sup>	1615	1650	1680	1593	1614	1631	1544	1551	1563
Thermal conductivity ( $\lambda_{eff}$ )	W/m·K	0.476	0.490	0.502	0.467	0.476	0.484	0.448	0.454	0.455
Firing Temperature	°C	970								
Bending strength/fired	Mpa	19.67	20.69	21.55	17.04	19.72	20.72	14.62	14.95	16.66
Body density	Kg/cm <sup>3</sup>	1621	1669	1690	1602	1626	1640	1552	1557	1572
Thermal conductivity ( $\lambda_{eff}$ )	W/m·K	0.478	0.498	0.506	0.471	0.480	0.486	0.451	0.452	0.459
Firing Temperature	°C	1000 *								
Bending strength/fired	Mpa	19.84	21.58	21.89	17.79	20.65	21.27	14.96	15.48	17.26
Body density	Kg/cm <sup>3</sup>	1631	1670	1700	1603	1629	1650	1556	1560	1579
Thermal conductivity ( $\lambda_{eff}$ )	W/m·K	0.482	0.498	0.510	0.471	0.482	0.490	0.452	0.454	0.462

\* Peak firing tested temperature in Celsius degrees

Based on the current study's experimental investigations, it was determined that expanded perlite has a positive effect on the thermal insulation properties of the final fired products but it decreases their strength.

The density of clay bricks is a parametrical factor which depends on the specific gravity of the clay mixture, method of manufacture, peak firing temperature and holding time in the peak temperature. The density results of the final products revealed three significant points, which are as follows:

1. Higher densities are obtained in higher peak temperatures;
2. Higher densities are obtained as the vacuum of the extruder increases;
3. Lower densities are achieved as the expanded perlite ratio is increased.

Higher peak temperatures showed higher densities and weight loss in the final products. Loss of weight under firing over 850 °C was attributed to the loss of organic matter

in clay. In addition, brick weight loss also depends on the inorganic substances in clay being fired.

In combination with the higher firing shrinkage and the lower absorption values which were presented at higher peak firing temperatures, the porosity of the final product seemed to be remarkably reduced. Porosity refers to air gaps in the body of the ceramic product and is interconnected with water permeability. Higher porosity showed higher absorption, lower density, and decreased strength.

The vacuum of the extruder during shaping was also shown to be a crucial parameter because less vacuum relates to lower body cohesion and more water presence in the samples. The formatting water was evaporated during the drying procedure by creating porosity (air gaps) which also resulted in the lower density of the final product.

As mentioned above, the density of expanded perlite is much lower than that of a clay material. The higher the ratio employed, the lower the final density.

According to EN1745, the body density of a fired clay product is related to the thermal conductivity coefficient ( $\lambda$  value). The thermal conductivity coefficient for samples with the same process environment (vacuum pressure and peak firing temperature) presented a 12.38% improvement with the addition of 30% expanded perlite for temperatures of over 900 °C and 10.12% for temperatures under 899 °C.

The mechanical strength, as expected, decreased with the addition of expanded perlite; however, even in the maximum tested amount of expanded perlite, the bending strength values were acceptable for brick production (more than 30 kg/cm<sup>2</sup> for the dry products and more than 100 kg/cm<sup>2</sup> for the fired products). The higher the vacuum used during extrusion, the higher the strength values, thereby indicating that extrusion is also a crucial parameter for the production environment in general.

## 5. Conclusions

It has become increasingly apparent that by adding expanded perlite to brick production clay mixtures, a structure with increased porosity and lower density can be achieved in the final product that leads to a decrease in the thermal conductivity coefficient and improved thermal insulation properties. The increase in porosity however is accompanied by the mechanical properties' degradation. In this study, expanded perlite was added to clay mixtures in percentages of 20 and 30 % wt and the products' properties were compared to the properties of bricks developed without the addition of perlite. The process parameters, i.e., the peak firing temperature and the vacuum employed during extrusion were also investigated in combination with the expanded perlite percentage.

It was found that the addition of perlite, when all the other parameters were kept constant, decreased the products' density by 2.9% to 7.1% and the thermal conductivity coefficient by 5.4% to 9.5%. These reductions became less pronounced as the peak firing temperature and the vacuum index employed during extrusion both reduced. However, as expected, the decrease in density and the increase in porosity had a negative effect on bending strength. Thus, as the perlite percentage increased, with the rest of the parameters being constant, the bending strength decreased by 18% to 28%, with the larger deviation being observed when the high vacuum index of 0.9 kp/cm<sup>2</sup> was employed. However, all the values obtained for the bending strength were well above the minimum accepted value (100 Kg/cm<sup>2</sup>).

Furthermore, the vacuum of the extruding of wet products for the same perlite–clay mixture was shown to significantly affect the final product. The higher the vacuum, the lower the porosity of the final product, making mixing with the expanded perlite not particularly advantageous for vacuum extrusion. Perlite appears to be crushed by the extrusion pressure of the clay material particles, which are much finer and do not contribute significantly to the improvement of the insulating properties. However, as the perlite percentage increases, the effect of vacuum becomes less important and does not affect results to a considerable degree.

Overall, by adjusting the processing parameters, the density of the final products can be reduced by up to 9.26%, the thermal conductivity by up to 12.83%, and the bending strength by up to 46%.

The above conclusion concerns the whole range of temperatures used in the experimental process. The use of expanded perlite can be particularly important in the manufacture of handmade bricks in which expanded perlite cannot be crushed and the density can be reduced significantly. Such a study seems particularly interesting, since from the data of the existing study it becomes obvious that less of a vacuum (i.e., the pressure of the molecules of the productive mixture) creates better insulating results. However, in such a study it would be important to monitor the decrease in the strength of the final product compared to the increase in the porosity of the material and efflorescence phenomenon [2,3].

Another future task within the scope of the research project “improvement of the thermal insulation in clay bricks with the addition of expanded additives” will concentrate on the following main targets: the consumption measurements of the necessary mixing water and of the firing procedure in comparison with the cost of expanded perlite for the brick industry.

**Author Contributions:** Conceptualization, I.M. and A.T.; methodology, I.M.; validation, I.M. and A.T.; formal analysis, I.M.; investigation, I.M.; resources, I.M.; data curation, I.M. and A.T.; writing—original draft preparation, I.M.; writing—review and editing, I.M. and A.T.; supervision, A.T. All authors have read and agreed to the published version of the manuscript.

**Funding:** “The APC was funded by 800 CHF by “COMPETITIVENESS, ENTREPRENEURSHIP & INNOVATION” (EPAvEK)” through NATIONAL ACTION: “RESEARCH-CREATE-INNOVATE SECOND CYCLE” as part of the project with Acronym MUDFIRE with work code T2EAK-03667.

**Institutional Review Board Statement:** Not applicable.

**Informed Consent Statement:** Not applicable.

**Data Availability Statement:** The data presented in this study are available on request from the corresponding author.

**Acknowledgments:** This study was performed as part of MUDFIRE Project no T2EAK-03667. The authors are grateful to SABO S.A. staff for providing details for a brick and tile industry operation and in particular the clay laboratory department for providing the extruding equipment and support for the experimental process environment of the study. We would like to express our gratitude to the XALKIS S.A. company for providing the clay material with the code TZ.

**Conflicts of Interest:** The authors declare no conflict of interest.

## References

1. Hamza, A.; Kocserha, I. The effect of expanded perlite on fired clay bricks. *J. Phys. Conf. Ser.* **2020**, *1527*, 01232. [[CrossRef](#)]
2. Foraboschi, P. Specific structural mechanics that underpinned the construction of Venice and dictated Venetian architecture. *Eng. Fail. Anal.* **2017**, *78*, 169–195. [[CrossRef](#)]
3. Foraboschi, P.; Vanin, A. Experimental investigation on bricks from historical Venetian buildings subjected to moisture and salt crystallization. *Eng. Fail. Anal.* **2014**, *45*, 185–203. [[CrossRef](#)]
4. Kocserha, I.; Kristály, F. Effects of Extruder Head’s Geometry on the Properties of Extruded Ceramic Products. *Mater. Sci. Forum.* **2010**, *659*, 499–504. [[CrossRef](#)]
5. Fediuk, R.S.; Yushin, A.M. The use of fly ash the thermal power plants in the construction. *IOP Conf. Ser. Mater. Sci. Eng.* **2015**, *93*, 012070. [[CrossRef](#)]
6. Bessmertnyi, V.; Lesovik, V.; Krokhin, V.; Puchka, O.; Nikiforova, E. The reducing effect of Argon in the plasma treatment of high-melting nonmetallic materials. *Glass Ceram.* **2001**, *58*, 362–364. [[CrossRef](#)]
7. Taurino, R.; Ferretti, D.; Bozzoli, F.; Bondioli, F. Lightweight clay bricks manufactured by using locally available wine industry waste. *J. Build. Eng.* **2019**, *26*, 100892. [[CrossRef](#)]
8. La Rubia-García, M.D.; Yebra-Rodríguez, Á.; Eliche-Quesada, D.; Corpas-Iglesias, F.A.; López-Galindo, A. Assessment of olive mill solid residue (pomace) as an additive in lightweight brick production. *Constr. Build. Mater.* **2012**, *36*, 495–500. [[CrossRef](#)]
9. Monteiro, S.N.; Vieira, C. On the production of fired clay bricks from waste materials: A critical update. *Constr. Build. Mater.* **2014**, *68*, 599–610. [[CrossRef](#)]
10. Sodeyama, K.; Sakka, Y.; Kamino, Y.; Seki, H. Preparation of fine expanded perlite. *J. Mater. Sci.* **1999**, *34*, 2461–2468. [[CrossRef](#)]

11. Sadik, C.; Albizane, A.; El Amrani, I. Production of porous firebrick from mixtures of clay and recycled refractory waste with expanded perlite addition. *J. Mater. Environ. Sci.* **2013**, *4*, 2028–2508.
12. Sedat, K.; Sabit, E.; Hikmet, G. Firing temperature and firing time influence on mechanical and physical properties of clay bricks. *J. Sci. Ind. Res.* **2006**, *65*, 153–159.
13. *ASTM D422-63*; Test Method for Particle-Size Analysis of Soils. ASTM International: West Conshohochen, PA, USA, 2007; pp. 19428–2959.
14. *ASTM D698-12*; Test Method for Laboratory Compaction Characteristics of Soil Using Standard Effort, Annual Book of ASTM Standards. ASTM International: West Conshohochen, PA, USA, 2014; pp. 19428–2959.
15. *ASTM D4318-17*; Standard Test Methods for Liquid Limit, Plastic Limit, and Plasticity Index of Soils, Annual Book of ASTM Standards. ASTM International: West Conshohochen, PA, USA, 2017; pp. 19428–2959.
16. Žurauskienė, R.; Mačiulaitis, R.; Petrikaitis, F. Usability of Lithuanian fusible clay for sintered ceramics. *J. Civ. Eng. Manag.* **2001**, *7*, 191–196. [[CrossRef](#)]
17. Andrade, F.; Al-Qureshi, H.; Hotza, D. Measuring the plasticity of clays: A review. *Appl. Clay Sci.* **2011**, *51*, 1–7. [[CrossRef](#)]
18. Händle, F. *Extrusion in Ceramics*, 1st ed.; Springer: Berlin/Heidelberg, Germany, 2007.
19. European Commission. COM 2007, 260. Reference Document on Best Available Techniques in the Ceramic Manufacturing Industry. Available online: <https://eippcb.jrc.ec.europa.eu/reference/ceramic-manufacturing-industry> (accessed on 30 March 2022).
20. *ASTM C326-09*; Standard Test Method for Drying and Firing Shrinkages of Ceramic Whiteware Clays, Annual Book of ASTM Standards. ASTM International: West Conshohochen, PA, USA, 2018; pp. 19428–2959.
21. *ASTM C373-14a*; Standard Test Method for Water Absorption, Bulk Density, Apparent Porosity, and Apparent Specific Gravity of Fired Whiteware Products, Ceramic Tiles, and Glass Tiles, Annual Book of ASTM Standards. ASTM International: West Conshohochen, PA, USA, 2014; pp. 19428–2959.
22. *ASTM C 648-20*; Standard Test Method for Breaking Strength of Ceramic Tile. ASTM International: West Conshohochen, PA, USA, 2020; pp. 19428–2959.
23. *BS EN 1745*; Masonry and Masonry Products— Methods for Determining Thermal Properties. British Standards Institution: London, UK, 2020.
24. Tsega, E.; Legessa, A. Effects of Firing Time and Temperature on Physical Properties of Fired Clay Bricks. *Am. J. Civ. Eng.* **2017**, *65*, 21–26. [[CrossRef](#)]